supplemental Figure 1

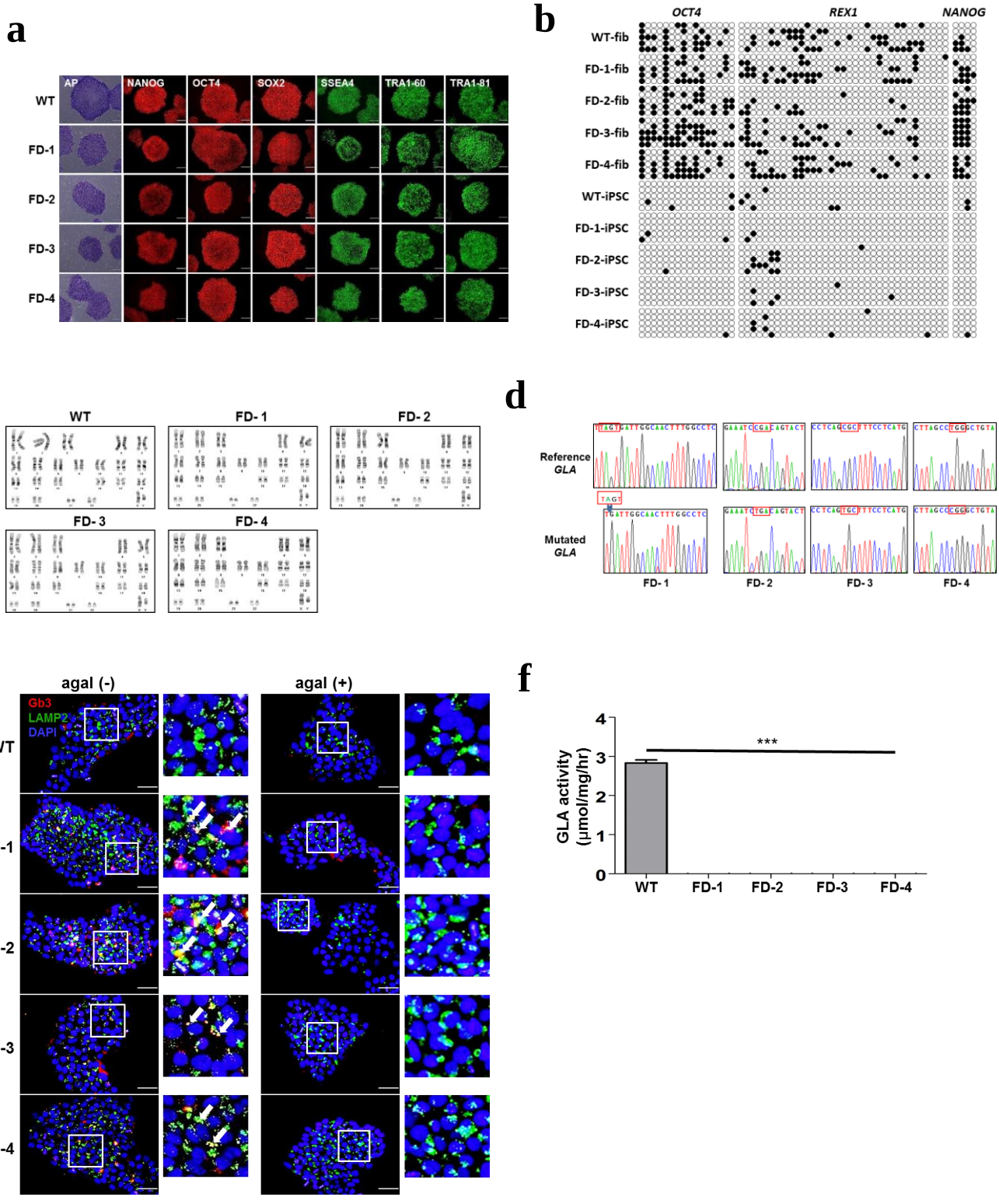

Figure S1. Characterizations of FD-iPSCs

(a) Expression of pluripotency-associated markers in WT- and FD-iPSCs. Like WT-iPSCs, FD-iPSCs are positive for AP activity and express pluripotent markers. Scale bar, 500 μm. AP, alkaline phosphatase. (b) Epigenetic reprogramming of FD-iPSCs. Promoters of pluripotency-associated genes are demethylated in FD-iPSCs derived from FD-fibroblasts. Each circle represents the methylation status of a single CpG dinucleotide: empty circle, unmethylated; filled circle, methylated. fib, fibroblasts. (c) Karyotypes of WT- and FD-iPSCs. Four karyotypically normal FD-iPSC lines. (d) Genetic mutations in FD-fibroblasts. (e) Accumulation of Gb3 in FD-iPSCs. Gb3 accumulation in FD-iPSCs not treated with agalsidase-ß (left panel). Treatment with agalsidase-ß reduces Gb3 accumulation in FD-iPSCs (right panel). Arrows represent Gb3 signal within lysosomes. LAMP2, a lysosomal marker. Scale bar, 50 μm. (f) A paucity of GLA activity in FD-iPSCs. As expected, FD-iPSCs show no GLA activity. The data are expressed as means ± SEM (n=3). *** $p < 0.001$. GLA, α-galactosidase A. WT, wild type. FD, Fabry disease.

supplemental Figure 2

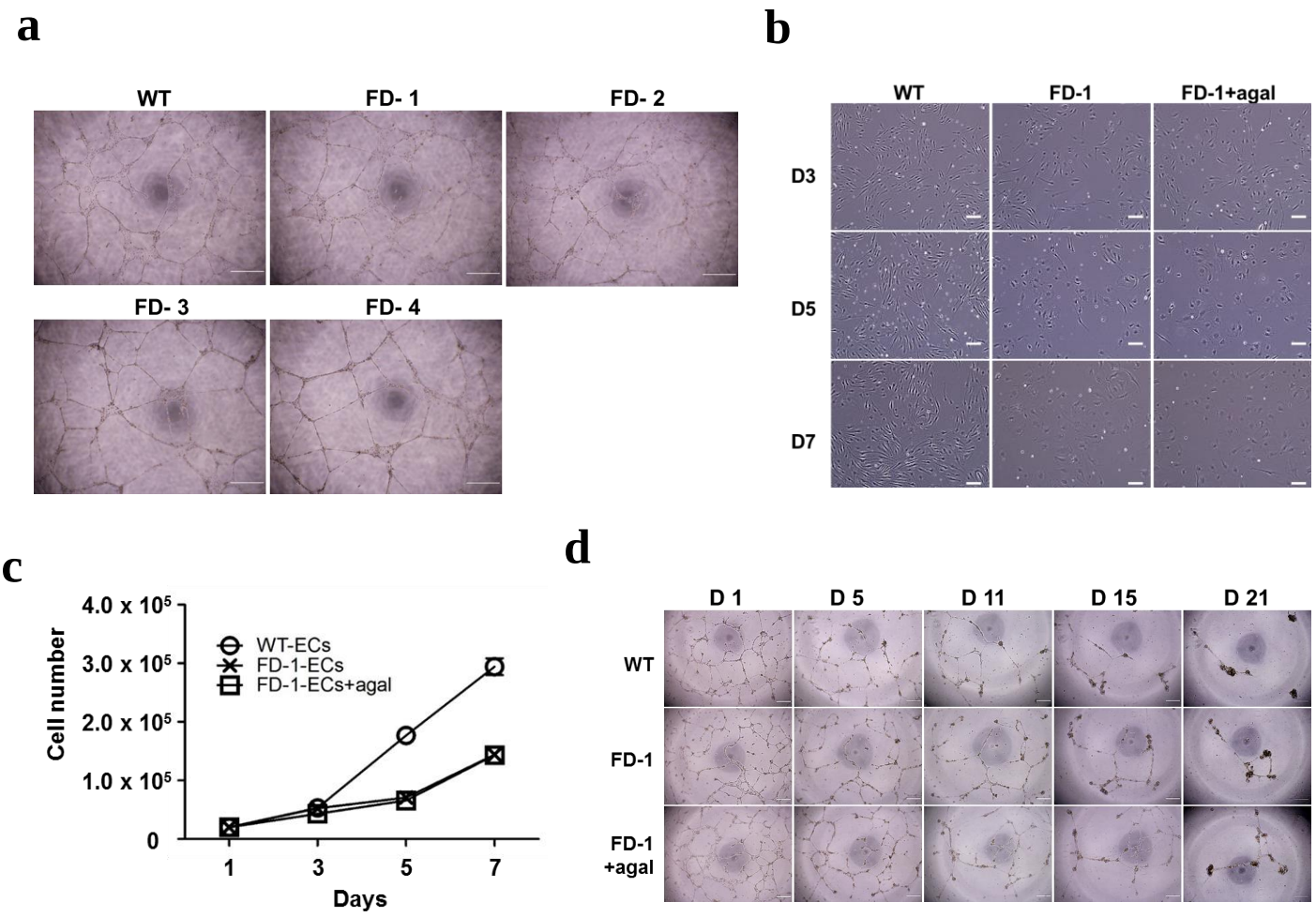

Figure S2. Functional characterization of FD-VECs, related to Figure 1.

(a) Tube formation assay of FD-VECs at an early stage of differentiation. FD-VECs at 3 days of EC development from isolated CD34+ progenitors form tube-like structures like WT-VECs. Scale bar, 100 μm. (b) Aberrant development of FD-1-VECs during in vitro culture. FD-1-VECs are morphologically normal after 3 d of culture, but their appearance changes after 5 or 7 d of culture. Similar anomalies appear in FD-1-VECs treated with agalsidase-ß (FD-1+agal). (c) Growth curves for WT- and FD-VECs. The data are expressed as means ± SEM (n=3). (d) Tubule maintenance in FD-VECs. The ability of FD-VECs to maintain tubules is similar to that of WT-VECs. Scale bar, 100 μm.

supplemental Figure 3

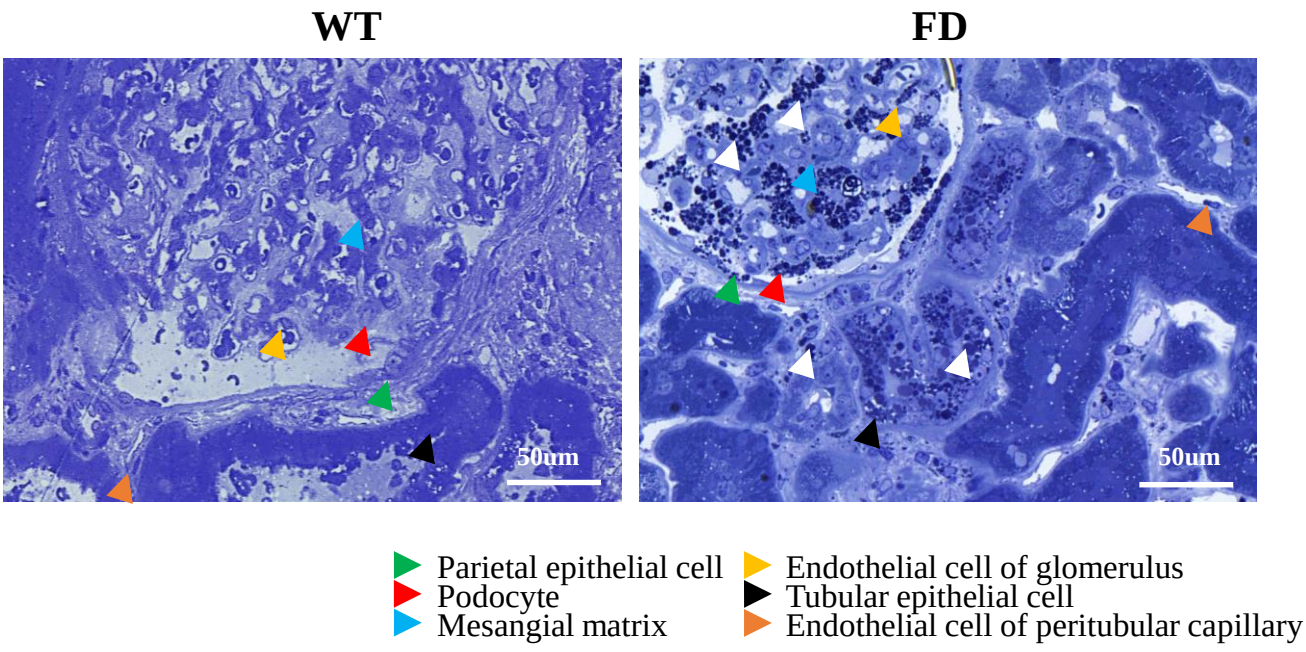

Figure S3.

Gb3 accumulation in renal tissues biopsied from FD patients. Toluidine blue staining of renal biopsies shows Gb3 accumulation in parietal epithelial cells, podocytes, mesangial matrix, glomerular endothelial cells, tubular epithelial cells, and peritubular capillary endothelial cells. Scale bar, 50 μm.

supplemental Figure 4

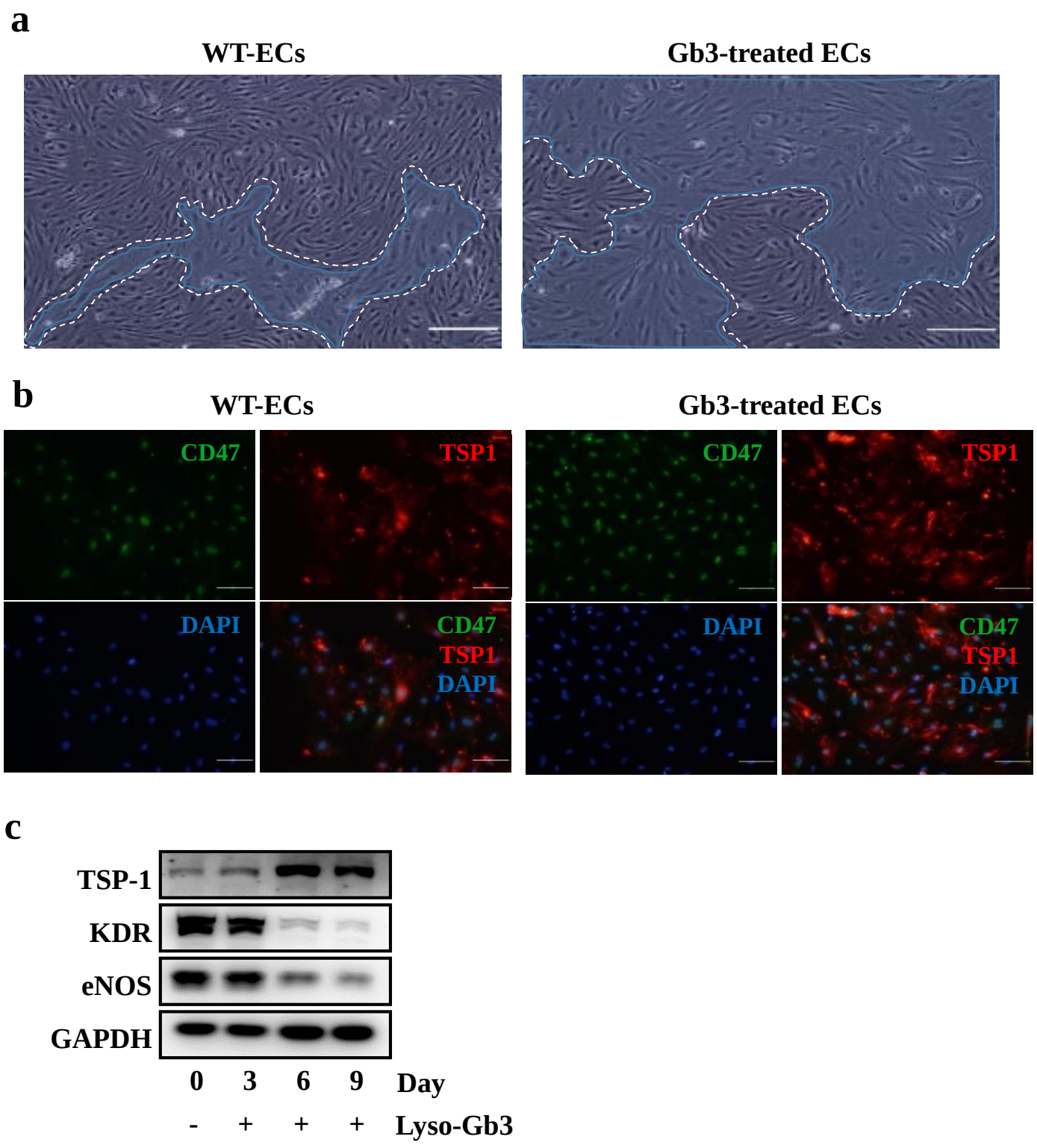

Figure S4. Effects of Lyso-Gb3 treatment on the development of WT-VECs

(a) Morphological changes in WT-VECs induced by Lyso-Gb3 treatment. When WT-CD34+ progenitors are treated with Lyso-Gb3 (400 nM) for 9 d, most of the resultant VECs are morphologically abnormal. Thus, the proportion of abnormal VECs expands in WT-VECs after GB3 treatment (light blue area within dashed line). Scale bar, 500 μm. (b) Immunostaining of TSP-1 in Lyso-Gb3-treated WT-VECs. Scale bar, 100 μm. (c) Effects of Lyso-Gb3 treatment in WT-VECs. A western blot analysis shows treatment with Lyso-Gb3 increases TSP-1 expression and decreases KDR and eNOS expression in WT-VECs. D, Day.

supplemental Figure 5

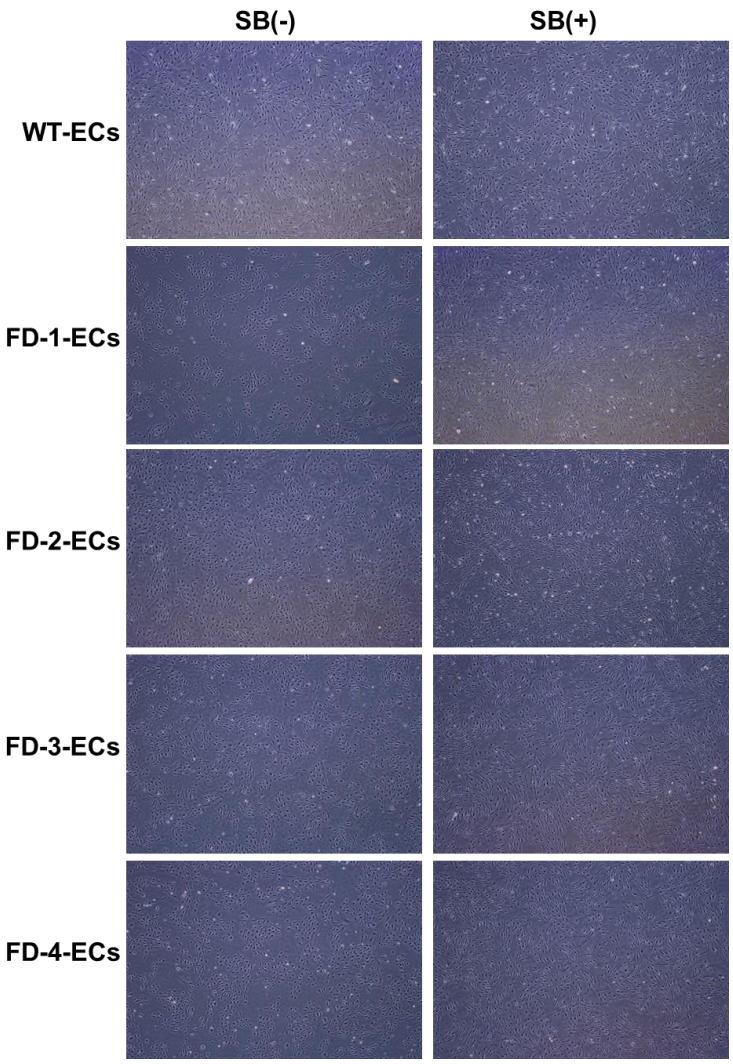

Figure S5. Morphological recovery of FD-VECs by inhibition of TGF-ß signaling.

supplemental Figure 6

a

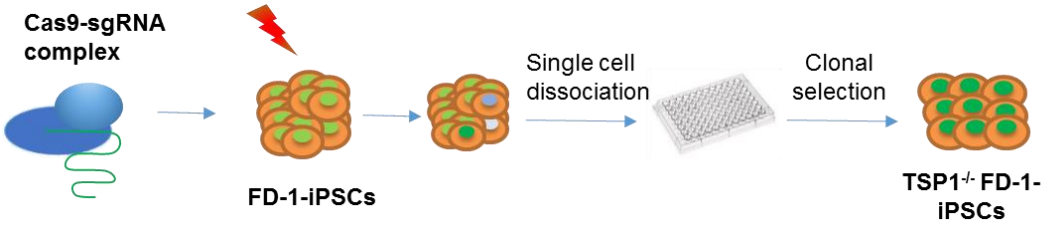

b

CRIPSR/Cas9 Target 1 (TSP-T1) 5'-GCAGCACGTGGTGTCTGTGGAAGAAGCTCTCCTGGCAACCGGCC-3'

CRIPSR/Cas9 Target 2 (TSP-T2) 5'-ACGCTGCTGGCCCTGGAGCGGAAAGACCACTCTGGCCAGGTCTT-3'

c

	Total reads	Insert	Deletion	Indel(%)
Cas9 alone	28429	0	9	9 (0.0%)
Cas9+T1_sgRNA	17769	117	1154	1271 (7.2%)

	Total reads	Insert	Deletion	Indel(%)
Cas9 alone	27483	0	3	3 (0.0%)
Cas9+T2_sgRNA	21243	198	1880	2078 (9.8%)

d

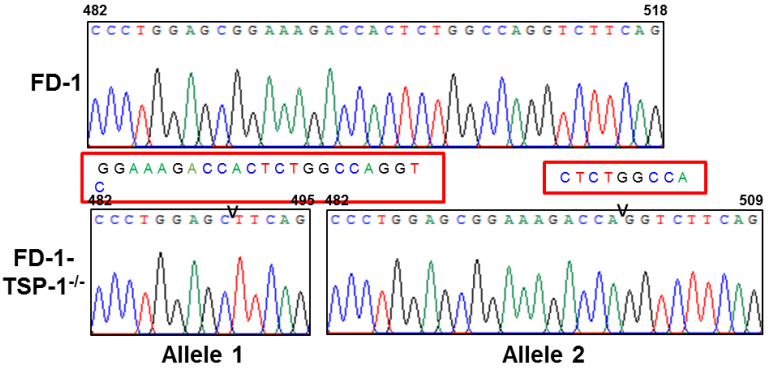

e

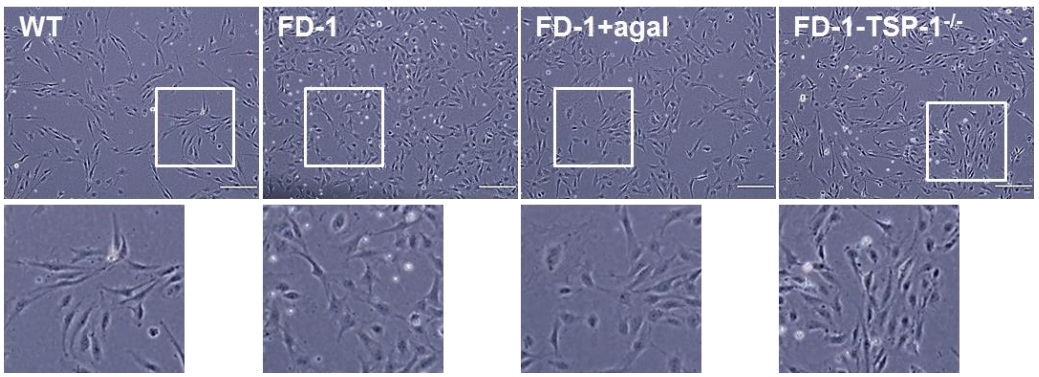

Figure S6. Generation of TSP-1$^{-/-}$FD-iPSCs using CRISPR/Cas9, related to Figure 5

(a) A schematic protocol for the generation of TSP-1$^{-/-}$FD-iPSCs using CRISPR/Cas9. Cas9-sgRNA complexes were introduced into single FD-1-iPSCs using electroporation. To obtain single clones, cells dissociated from the colonies formed after electroporation were placed individually in the wells of 96-well plates. (b) Two *THBS1*-specific target sequences containing sgRNA (underline) and PAM sequences (TGG in red). (c) Indel frequencies for two TSP-1-targeting sgRNAs. (d) Mutated *THBS1* sequences from FD-iPSCs. Using the CRISPR/CAS9 system, 23 and 9 nucleotides from Exon 3 of the *THBS1* gene in FD-iPSCs were deleted in allele 1 and allele 2, respectively. These were then designated FD-1-TSP-1$^{-/-}$ iPSCs. (e) Representative images of iPSC-derived VECs. Morphological rescue of VECs was observed in FD-1-TSP-1$^{-/-}$ VECs. Scale bars, 500 μm.

supplemental Figure 7

a

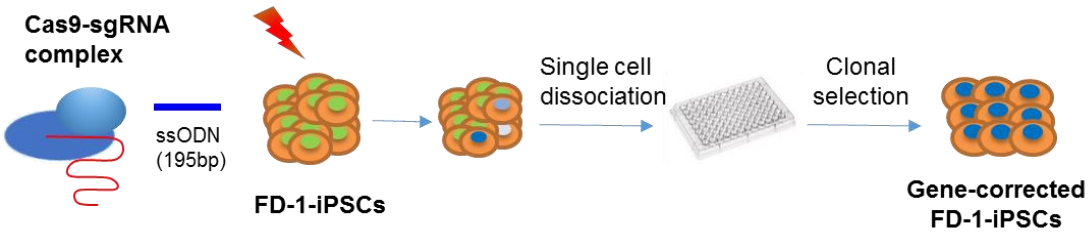

b

CRIPSR/Cas9 Target 1 (GLA-T1) 5'-TTATTTCATTCTTTTTCTCAGT----GATTGGCAACTTTGGCCTCAG-3'

CRIPSR/Cas9 Target 2 (GLA-T2) 5'-TTATTTCATTCTTTTTCTCAGT----GATTGGCAACTTTGGCCTCAG-3'

Donor ssODN (195mer) 5'-GAATTATTTCATTCTTTTTCTCAGTTGGTCATAGGGAACTTTGGCCTCAGCT-3'

c

	Total reads	Insert	Deletion	Indel(%)	HDR(%)
Cas9 alone	23233	0	3	3 (0.0%)	0 (0.0%)
Cas9+T1_sgRNA	22041	0	0	0 (0.0%)	0 (0.0%)
Cas9+T1_sgRNA+ssODN	24833	0	0	0 (0.0%)	0 (0.0%)

	Total reads	Insert	Deletion	Indel(%)	HDR(%)
Cas9 alone	23226	0	13	13 (0.1%)	0 (0.0%)
Cas9+T2_sgRNA	22636	339	2716	3055 (13.5%)	0 (0.0%)
Cas9+T2_sgRNA+ssODN	21316	1318	1766	3084 (14.5%)	877 (4.1%)

d

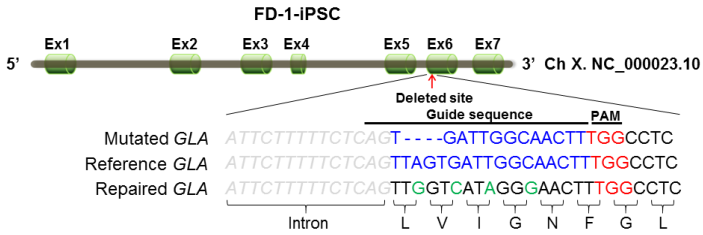

e

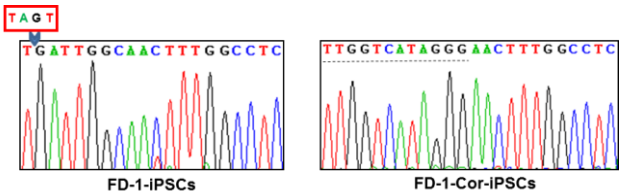

f

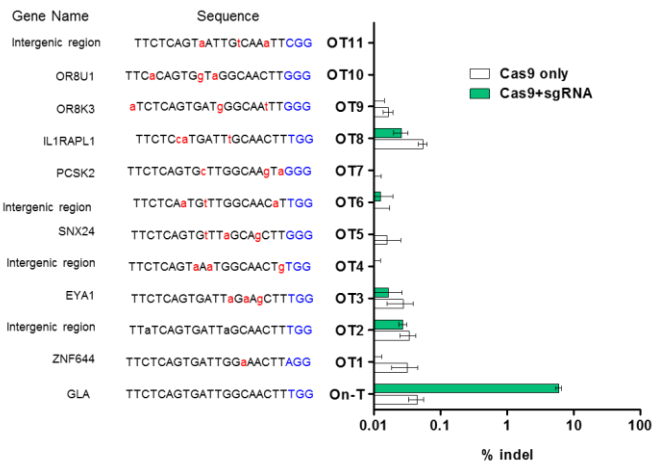

Figure S7. Generation of FD-1-Cor-iPSCs using CRISPR/Cas9, related to Figure 6

(a) Protocol for the correction of the *GLA* gene in FD-1-iPSCs using CRISPR/Cas9. (b) Two mutated GLA target sequences (GLA-T1 and GLA-T2), a PAM sequence (TGG), and an ssODN as a donor DNA. (c) Indel frequencies and HDR rates for each sgRNA. (d) Schematic representation of the gene-targeting strategy of mutated *GLA* genes using the CRISPR/CAS9 system. Four silent mutations were inserted into FD-1-iPSCs to discriminate them from the WT alleles after gene editing. (e) Confirmation of *GLA* gene correction by Sanger sequencing. The FD-1-Cor-iPSCs contained four silent mutations (dashed line). (f) Indel frequencies for the GLA-targeting sgRNA (GLA-T2) at potential off-target sites identified using Cas-OFFinder. Mismatched nucleotides (red) and PAM sequences (blue) are denoted in their respective potential off-target sites.

supplemental Figure 8

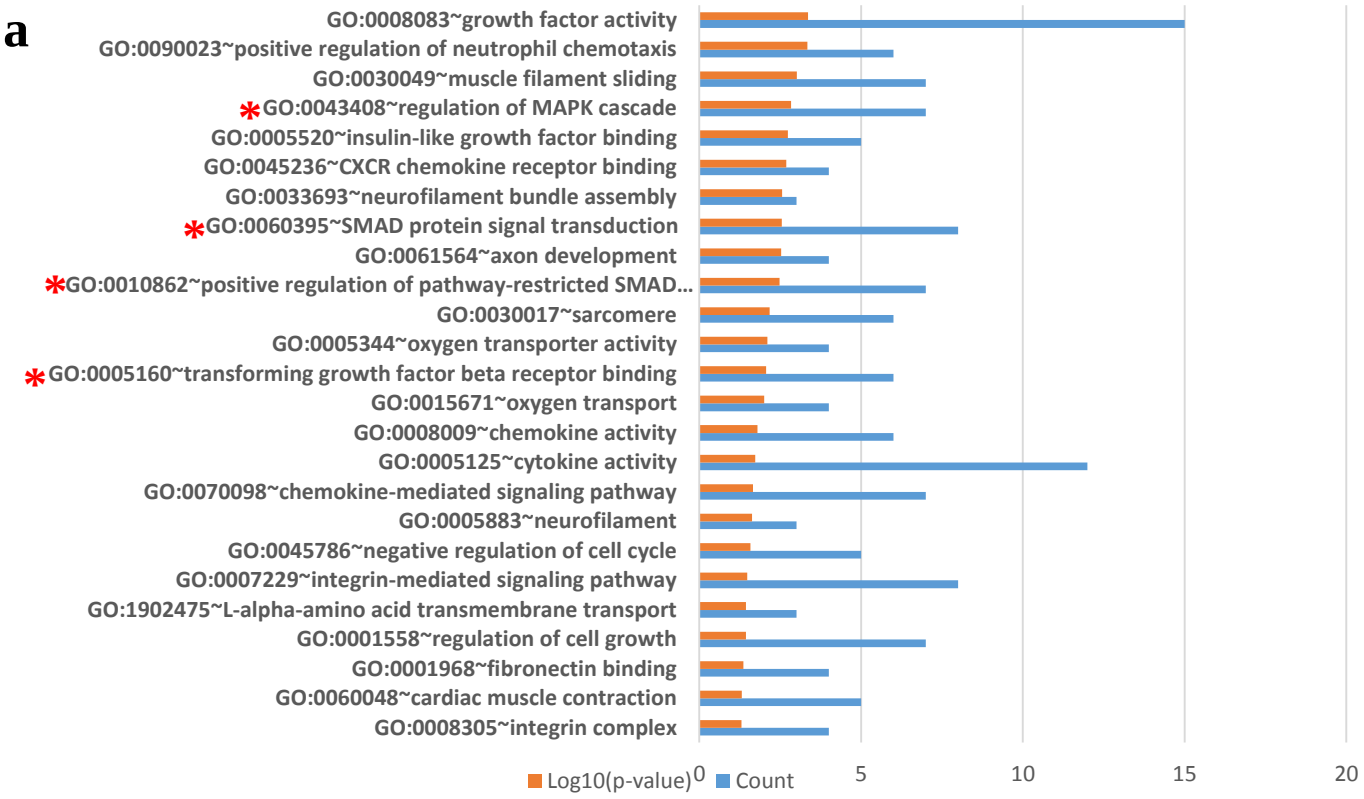

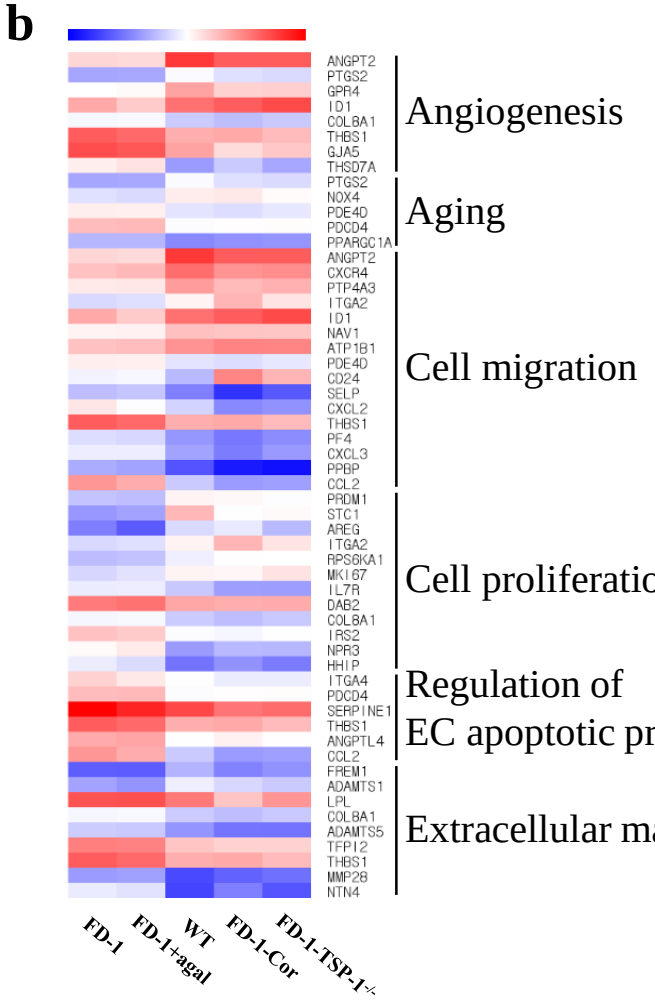

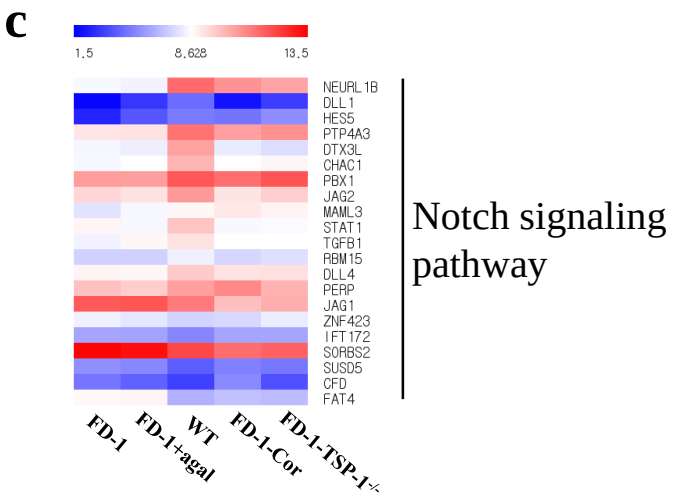

Figure S8.

(a) Comparison of GO terms associated with FD-1-VECs and WT-VECs. Red stars indicate enriched GO terms related to the TGF-β signaling pathway. (b) Heat map for significant transcriptional changes in cell function-associated genes. (c) Heat map for significant transcriptional changes in Notch signaling.